Particle in Cell realistic mass ratio simulations of magnetic reconnection with the semi-implicit adaptive Multi Level Multi Domain method

M.E. Innocenti[1], A. Beck[2], T. Ponweiser[3] S. Markidis[4], G. Lapenta[1]

[1] *KULeuven (University of Leuven), 3001 Leuven , Belgium*

[2] *Laboratoire Leprince-Ringuet, CNRS-IN2P3, France*

[3] *RISC Software GmbH, Hagenberg, Austria*

[4] *KTH Royal Institute of Technology, Stockholm, Sweden*

Particle In Cell (PIC) simulations of space plasmas are often prohibitively computationally expensive due to the need to simulate large domains (in the case of magnetic reconnection in space [3], tens or hundreds of ion skin depths d_i per side) with at least local very high resolution, sometimes in cases with very high mass ratio m_r between the particle species. Realistic mass ratios make simulations of reconnection more challenging, if the electron scales have to be resolved, due to the scaling of the skin depths d_s and plasma frequencies ω_{ps} with the mass ratio (s is the particle species): $d_i/d_e = \omega_{pe}/\omega_{pi} = \sqrt{m_r}$, under the assumption of identical density for the species. The recently developed Multi Level Multi Domain method (MLMD [8, 1]), an Implicit Moment Method [10] adaptive technique for PIC simulations, promises to reduce the computing cost of these simulations by representing the domain as a collection of different *grids* or *levels* resolved with different spatial and (recently [7]) temporal resolutions. If high resolution is needed only in a reduced fraction on the entire domain, computing resources are saved by simulating only that as a highly resolved "refined grid RG", while the rest of the domain is solved with a suitable coarser resolution ("coarse grid CR"). The savings in the execution times of such simulations, compared to "normal" cases where the same, high resolution is used everywhere, are remarkable, going as high as 70 times when a high Refinement Factor such as $RF = 14$ is used [1]. The Refinement Factor is the jump in spatial resolution between the grids . Here, a realistic mass ratio simulation of magnetic reconnection is used to demonstrate the potentialities of the the MLMD method: it will be shown that large scale and small scale dy-

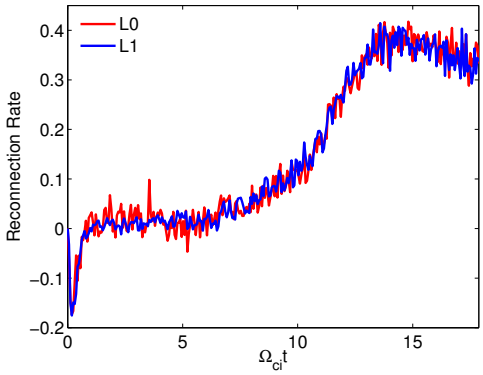

Figure 1: *Reconnection Rate on the coarse (red line) and refined (blue line) level as a function of time.*

namics are captured *together by the same simulation using a relatively low number of cells*. A domain with size $L_{x,g_0} \times L_{y,g_0} = 60\ d_i \times 30\ d_i$ (where g_0 identifies the CG) is simulated at the coarser level with spatial resolution $dx_{g_0} = 0.059\ d_i = 2.51\ d_e$, adequate to represent ion-scale processes but incapable of reproducing electron-scale dynamics, which occur on scales of fractions of the electron skin depth.

A double Harris equilibrium [6] is used at initialization, with the following parameters: half-width of the current sheet $L_H/d_i = 0.53$, electron thermal velocity $v_{th,e}/c = 0.045$, where c is the speed of light, $m_r = 1836$ and temperature ratio between ions and electrons $T_i/T_e = 20$. An ion and electron background with density $1/10$ of the streaming particles is added. Two reconnection X-points are initialized through a perturbation at coordinates $x/d_i = L_{x,g_0}/4$, $y/d_i = L_{y,g_0}/4$ ("control" reconnection point) and $x/d_i = 3/4\,L_{x,g_0}$, $y/d_i = 3/4\,L_{y,g_0}$. The second X-point is simulated also with a RG centered around it and having extension $L_{x,g_1} \times L_{y,g_1} = 60/RF\ d_i \times 30/RF\ d_i$ (g_1 identifies the RG), where $RF = 14$. The same number of cells is used in the coarse and in the RG, giving $dx_{g_1} = 0.0042\ d_i = 0.18\ d_e$, sufficient to fully capture electron scale dynamics on the RG. The same time step $\omega_{pi}t = 0.09$, with ω_{pi} the ion plasma frequency, and 196 particles per species per cell are used at both levels. The ion-scale evolution of the two grid levels is the same, as proved by the fact that the reconnection rate (which is not sensitive to electron-scale dynamics [2]), shown in Fig. 1, evolves in the same way with time on the two levels. Fig. 1 also attests that the grid interlocking activities described in [8] (field and particle boundary condition exchange from the coarse to the RG, refined field projection from the refined to the CG) satisfactorily couple the grid evolution at the different levels.

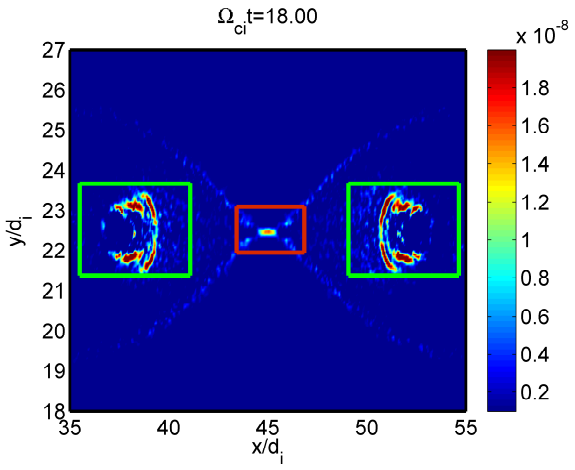

Figure 2: $\mathbf{J}_{el} \cdot \mathbf{E}$ *metric at time* $\Omega_{ci}t = 18.00$ *on a fraction of the coarse grid,* $35 < x/d_i < 55$, $18 < y/d_i < 27$. *The inner EDR and the Dipolarization Fronts are highlighted by red and green rectangles.*

Fig. 2 allows to appreciate the large scale evolution of reconnection as sampled, at ion-scale resolution, by the CG. $\mathbf{J}_{el} \cdot \mathbf{E}$ is there shown at time $\Omega_{ci}t = 18.00$ in a fraction of the CG, $35 < x/d_i < 55$, $18 < y/d_i < 27$, enclosing the reconnection point resolved also with higher resolution. Ω_{ci} is the ion cyclotron frequency, $\mathbf{J}_{el}$ the electron current and $\mathbf{E}$ the electric field. When $\mathbf{J}_{el} \cdot \mathbf{E} > 0$, work is being performed by the electric field on the electrons: these areas, mainly

the inner Electron Diffusion Region (EDR, highlighted by a red rectangle [5]) and the Dipolarization Fronts (green rectangles [9]), need electron scale resolutions to be properly investigated. We compare here aspects of EDR evolution as captured by the two grids. Fig. 3 shows a vertical cut of the Hall field E_y (blue line, left vertical axis) and of the $\mathbf{J}_{el} \cdot \mathbf{E}$ metric (red line, right vertical axis) as a function of y/d_i at time $\Omega_{ci}t = 12.48$, before the peak of reconnection is reached, on the refined (top panel) and coarse (bottom panel) grid at the x coordinate of the X-point, $x_{g1}/d_i = 44.9979$ and $x_{g0}/d_i = 44.9853$ respectively. Notice that the RG correctly captures both the vertical variation of the Hall field (positive and negative at the lower and upper EDR boundary respectively) and the formation of an inversion layer *within* the EDR, the electric field signature of an electron hole in the v_y vs. y phase space originated by the meandering motion of electrons in the EDR [4]. As expected from [4], the inversion layer is more visible during the explosive phase of reconnection (before the reconnection peak is reached at $\Omega_{ci}t \approx 13$ in Fig. 1) and tends to decline when the plasma inflow is reduced. The CG, instead, as already pointed out in Fig. 8 in [1], does not show this kind of behavior: the peak value of the Hall field is reduced with respect to the RG due to the different resolution and the different spatial reach of the smoothing operations on the different grids (refer to [7] for an in-depth discussion) and no signs of the inversion layer are visible. Similar conclusions may be derived regarding the vertical extension of the EDR as measured by the two grids following the already mentioned $\mathbf{J}_{el} \cdot \mathbf{E} > 0$ criterium (incidentally, also the peak of $\mathbf{J}_{el} \cdot \mathbf{E}$ is lower and the bifurcation registered at the refined level is not captured when the resolution is lower, in the bottom panel). The RG yields an EDR half-width of $\delta y_{g1}/d_e = 2.36$, compatible with previous measurements, while the value calculated on the CG is $\delta y_{g0}/d_e = 6.21$, definitively larger due to the lower res-

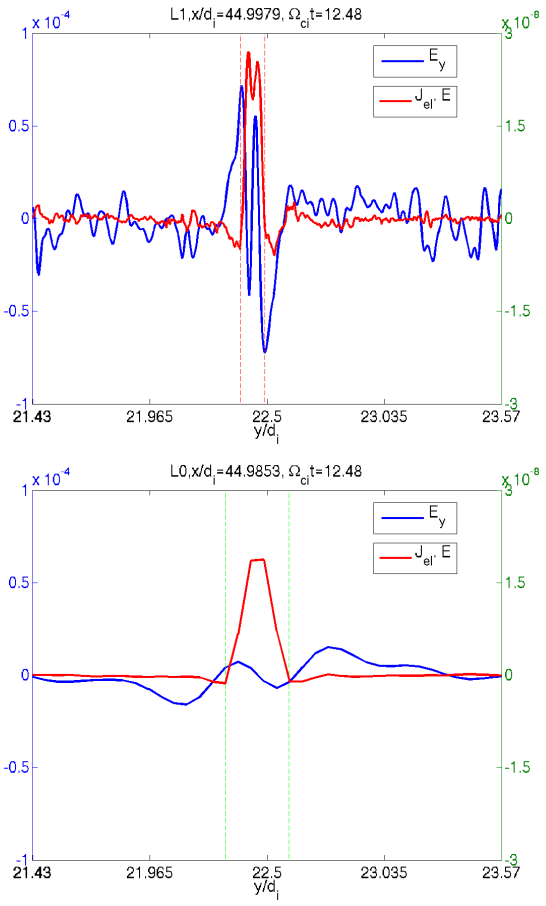

Figure 3: *Hall field E_y (blue line, left vertical axis) and $\mathbf{J}_{el} \cdot \mathbf{E}$ metric (red line, right vertical axis) as a function of y/d_i at time $\Omega_{ci}t = 12.48$ at the x coordinate of the X-point, $x_{g1}/d_i = 44.9979$ and $x_{g0}/d_i = 44.9853$ respectively. The red ($x_{g1}/d_i = 22.38$ and $x_{g1}/d_i = 22.49$) and green ($x_{g0}/d_i = 22.31$ and $x_{g0}/d_i = 22.60$) lines mark the vertical extension of the EDR in the refined and coarse grid respectively.*

olution: the entire EDR vertical extension measured on the RG is covered by less then 2 points on the coarse grid, by 26 points on the refined grid.

We have shown here a realistic mass ratio simulation of magnetic reconnection performed with the recently developed MLMD method with the aim of highlighting the complementary roles of the coarse and refined grid in the MLMD system. The coarse grid reproduces the macroscopic evolution (e.g., Dipolarization Front expansion), while the smaller scales are simulated, in a reduced part of the domain, by the refined grid alone. It is reminded that employing the refined grid resolution on the the entire domain would require to use $(1024 \times 14) \times (512 \times 14)$ cells, rather than the $1024 \times 512 \times 2$ employed here, and would deliver comparable levels of results in the area where electron scale resolution is needed, the EDR. Future work will focus on resolving with electron scale resolution also the other area identified as interesting at the electron scales by the EDR criterium (Fig. 2), the Dipolarizarion Fronts.

This work has received funding from the European Union Seventh Programme for Research, Technological Development and Demonstration under Grant Agreement No 284461 - Project eHeroes (www.eheroes.eu).

References

[1] A. Beck, M.E. Innocenti, G. Lapenta, and S. Markidis. *JCP*, (0):–, 2013.

[2] J. Birn, J. F. Drake, M. A. Shay, B. N. Rogers, R. E. Denton, M. Hesse, M. Kuznetsova, Z. W. Ma, A. Bhattacharjee, A. Otto, and P. L. Pritchett. *JGR: Space Physics*,106(A3):3715–3719, 2001.

[3] D. Biskamp. *Magnetic reconnection in plasmas*, Cambridge University Press, 2005.

[4] Li-Jen Chen, William S Daughton, Bertrand Lefebvre, and Roy B Torbert. *PoP*, 18(1):012904, 2011.

[5] W. Daughton, J. Scudder, and H. Karimabadi. *PoP*, 13:072101, 2006.

[6] E. Harris. *Il Nuovo Cimento (1955-1965)*, 23:115–121, 1962.

[7] M. E. Innocenti, A. Beck, T. Ponweiser, S. Markidis, and G. Lapenta. in preparation.

[8] M.E. Innocenti, G. Lapenta, S. Markidis, A. Beck, and A. Vapirev. *JCP*, 238(0):115 – 140, 2013.

[9] A. Runov, V. Angelopoulos, M. I. Sitnov, V. A. Sergeev, J. Bonnell, J. P. McFadden, D. Larson, K.-H. Glassmeier, and U. Auster. *GRL*, 36(14):n/a–n/a, 2009.

[10] HX Vu and JU Brackbill. *CPC*, 69(2):253–276, 1992.